Changes in upper mesospheric and lower thermospheric temperatures caused by energetic particle precipitation

H. Nesse Tyssøy,[1,2] J. Stadsnes,[2] M. Sørbø,[2] C. J. Mertens,[3] and D. S. Evans[4]

Received 10 March 2010; revised 28 May 2010; accepted 29 June 2010; published 26 October 2010.

[1] A statistical evaluation on the upper mesospheric and lower thermospheric temperature effects caused by energetic particle precipitation is performed on the basis of data from the Thermosphere Ionosphere Mesosphere Energetics and Dynamics (TIMED) and NOAA 15, 16, and 17 satellites. By combining particle measurement from the medium energy proton and electron detectors (MEPED) on board the NOAA satellites, maps of the global particle precipitation can be obtained close in time to the SABER (Sounding of the Atmosphere using Broadband Emission Radiometry) temperature retrieval. Using large data sets, sorted by season, local time, and geomagnetic latitude, we investigated whether there are significant temperature effects in the upper mesosphere and lower thermosphere associated with the energetic particle precipitation. During both May/June and October/November 2003, we found a temperature increase related to particle precipitation at all heights above 100 km. In general, we did not find a consistent immediate temperature modification below 100 km associated with increased particle flux. Considering the temperatures retrieved during the extraordinary large geomagnetic storms in late October 2003, we found a cooling effect associated with energetic particle precipitation.

Citation: Nesse Tyssøy, H., J. Stadsnes, M. Sørbø, C. J. Mertens, and D. S. Evans (2010), Changes in upper mesospheric and lower thermospheric temperatures caused by energetic particle precipitation, *J. Geophys. Res.*, *115*, A10323, doi:10.1029/2010JA015427.

1. Introduction

[2] The energy budget in the upper mesosphere and lower thermosphere is poorly understood. A large number of parameters, such as electromagnetic radiation from the sun, particle precipitation, Joule heating, atmospheric waves, winds, turbulence, chemical reactions, infrared cooling, photoelectrons, and heat conduction all influence the energy budget. The energy balance is further complicated when taking into account the complex interaction of the different processes and that many of them are able to heat the atmosphere as well as cool it, depending on the specific conditions present [*Offermann*, 1985; *Roble*, 1995].

[3] During geomagnetic disturbances, the atmosphere experiences an energy increase from particle precipitation and Joule heating [*Banks*, 1977, 1979; *Rees et al.*, 1983]. At the same time, the particle precipitation influences the composition of the atmosphere through ionization, dissociation, and excitation. Changing the gas composition also changes the absorption of solar radiation, the chemical heating rates, and the infrared cooling rates. The plasma flow, controlled by the electric field and the new temperature gradients, changes the neutral winds, which in turn also modify the temperature and gas composition of the upper atmosphere. Intuitively, the energy supply from geomagnetic sources and the energy redistribution is expected to result in a temperature increase in the thermosphere and upper mesosphere. However, upper mesospheric temperature observations have shown apparent cooling, heating, or no measurable temperature changes coinciding with particle precipitation events [e.g., *Lastovicka*, 1988; *Zadorozhny et al.*, 1994; *von Savigny et al.*, 2007; *Pancheva et al.*, 2007; *Nesse Tyssøy et al.*, 2008].

[4] The contradictory results in the upper mesosphere may be due to the complexity of the energy budget, which makes it very difficult to determine the influence from just a single process in a case study. A large number of measurements, on the other hand, might average out the effects from some of the processes, such as tides and waves, making it easier to see whether there are any significant temperature effects from, e.g., energetic particle precipitation. In this paper, we combine temperature measurement from SABER on board the Thermosphere Ionosphere Mesosphere Energetics and Dynamics (TIMED) satellite, and particle measurement from medium energy proton and electron detectors (MEPED) on board NOAA/POES (National Oceanic and Atmospheric Administration/Polar Orbiting Environmental Satellites) 15, 16, and 17. By interpolating between the passes of the NOAA satellites, we obtain an estimate of the distribution of the precipitating particles in the area where SABER retrieves the temperature. Using large data sets, sorted by season, local time, and geomagnetic latitude, we investigate whether there

[1]The Royal Norwegian Naval Academy, Bergen, Norway.
[2]University of Bergen, Bergen, Norway.
[3]NASA Langley Research Center, Hampton, Virginia, USA.
[4]NOAA Space Environment Center, Boulder, Colorado, USA.

0148-0227/10/2010JA015427

Table 1. An Overview of the Four MEPED Energy Channels Used in This Paper, Along With the Altitude Range Where The Particles Deposit Most of Their Energy When Precipitating in the Atmosphere

MEPED energy channels	Altitude range
Protons 30–80 keV	110–140 km
Protons 80–250 keV	100–130 km
Protons 250–800 keV	90–110 km
Electrons >30 KeV	<105 km

are significant upper mesospheric temperature effects associated with the energetic particle precipitation. As the qualitative temperature response in the lower thermosphere is known to be heating, we may use the temperature response above 100 km to validate our technique.

2. Instrumentation

2.1. TIMED/SABER

[5] In 2001, TIMED was launched into a 625 km circular polar orbit, with 71° inclination. The orbit period is about 97 minutes. TIMED's payload consists of four instruments, including the infrared radiometer SABER.

[6] SABER is measuring infrared emissions at 10 different wavelength bands. We focus on measurements made around 15 μm, a vibrational transition band of CO_2, which can be used to estimate the neutral temperatures up to about 130 km. The instrument points perpendicularly to the orbit direction, and every 60 days the look direction is changed by 180° to maintain a certain temperature in the instrument. Due to SABER's viewing direction, it does not cover both the southern and northern auroral oval in the same time period.

[7] The effective vertical resolution of the retrieved SABER data products is approximately 2 km. The retrieved temperature profiles from 80 to 100 km altitude represent an average over the horizontal line of sight of ±150 km and a cross-path distance of ±70 km taking into account the movement of the satellite. As a result, retrieved temperatures in the height interval 80–120 km at a given tangent height represent an average over an atmospheric volume of 300 km × 140 km × 2 km.

2.2. NOAA/MEPED

[8] The NOAA/POES spacecraft are part of NOAA's operational weather satellite system. In 2003, the year this study is based upon, three satellites, NOAA 15, 16, and 17 were orbiting the Earth in a polar, sun-synchronous orbit at 850 km altitude with a period of approximately 100 minutes. Each satellite carries two types of particle sensors, Total Energy Detector (TED) and MEPED [*Evans and Greer*, 2000].

[9] MEPED provides directional measurements of energetic particles. The instrument holds four directional solid-state detectors mounted in groups of two, pointing 9° and 89° to the local vertical. We refer to these detectors as the vertical and horizontal detector, respectively. At high latitudes, the vertical detector measures the particles in the loss cone, while the horizontal detector measures particles that mirror or are close to mirroring at satellite altitude. The detectors have a 30° total field of view. The protons are measured in six energy ranges: 30–80, 80–250, 250–800, 800–2500, 2500–6900, and >6900 keV. The electrons are measured in three energy channels: >30, >100, and >300 keV. We focus on the particles measured by MEPED which deposit most of their energy in the altitude range 90–120 km as shown in Table 1.

3. Observations

[10] SABER retrieves a vertical profile of the temperature once every minute. Ideally, we would like to know the flux of precipitating energetic particles at the exact height and in the actual region prior to and when SABER is measuring. Using particle measurements from the vertical detector on the MEPED instruments onboard NOAA 15, 16, and 17, we can detect the precipitating particles in and near our region of interest close in time to the SABER observations. The particle measurements are projected down to about 100 km, where they are sorted into a geomagnetic grid, where each cell covers 4° in latitude and 10° in longitude. A global distribution of the precipitating energetic particles is then obtained by interpolating linearly between cells at the same geomagnetic latitudes for the passes of the different satellites. For this interpolation to be a valid estimate of the particle precipitation where SABER is measuring, we require that all three NOAA satellites have left the region of interest before SABER is entering the region. Global patterns of precipitating particle fluxes based on the NOAA satellites using interpolation techniques have been generated before by, e.g., *Fang et al.* [2007].

[11] The temperature measurements are sorted into the same geomagnetic grid as used for the particle measurements. The geomagnetic grid size is larger than the horizontal resolution of the retrieved temperatures at latitudes where particle precipitation occurs.

[12] Considering the interpolation, the time delay, and the complicated energy budget, we do not expect a perfect correlation between a possible temperature modification and the corresponding particle precipitation. However, if the energetic particles influence the temperature at the chosen horizontal scale, we do expect to see temperature trends if we have a sufficient amount of data. By significant temperature change in this context, we mean a temperature difference that exceeds the sum of the respective standard deviations of the temperature profiles we compare.

[13] In the following, we use a total amount of 80 days of TIMED/SABER and NOAA/MEPED data covering two time periods: May/June and October/November 2003. We only use data from the northern hemisphere as SABER's viewing direction only covers the northern auroral oval in these time periods. However, large particle fluxes associated with the storm time periods are not distributed evenly throughout our 40-day periods. This means that the temperature profiles coinciding with large particle fluxes are not necessarily distributed as evenly throughout our local time interval as the quiet time temperature profiles. To ensure that we do not introduce a systematic temperature effect associated with the temperature climatology and the phasing of the temperature sampling, we sort the temperatures into 1 hr local time intervals and calculate the average temperature within each 4° geomagnetic latitude interval associated with a specific particle flux level. This gives a ΔT ($\Delta T = \overline{T}_{elevatedfluxlevels} - \overline{T}_{lowfluxlevels}$) for each local time hour and

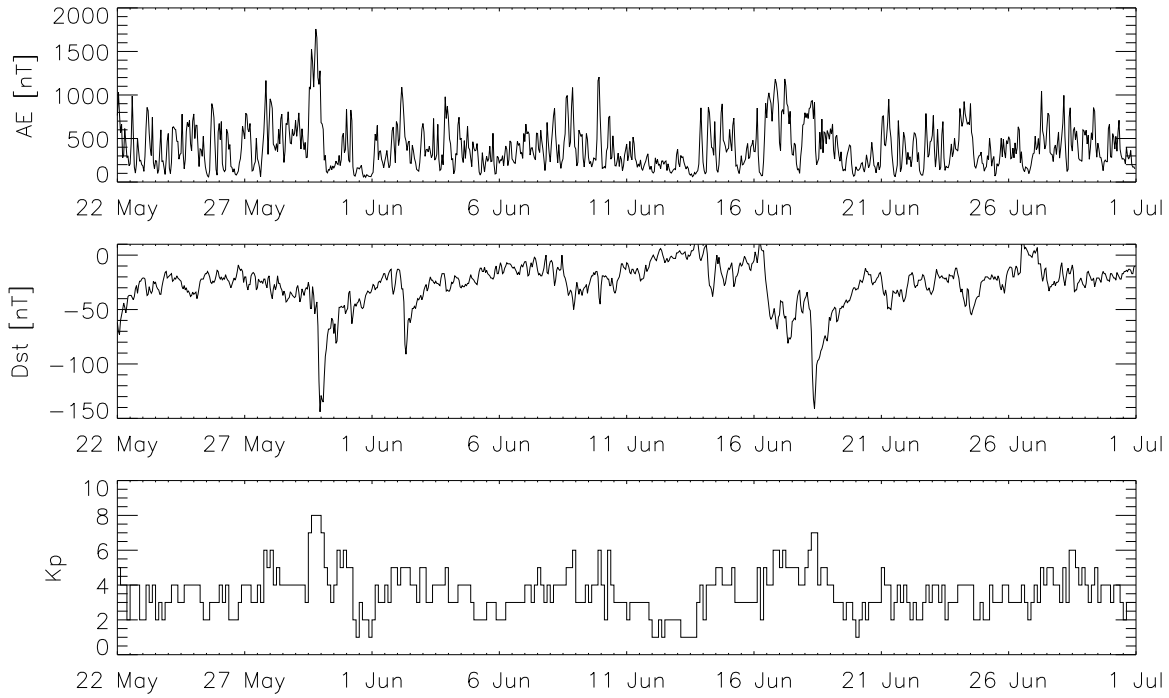

Figure 1. Hourly AE and Dst (upper and middle plot), and 3-hourly Kp (bottom plot) for the period 22 May–30 June 2003.

geomagnetic latitude interval. Since the number of temperature profiles the $\overline{T}_{elevatedfluxlevels}$ is based on depends on the SABER coverage during the periods of particle fluxes, we should be careful in interpreting two different ΔTs as different local time responses. However, the average temperature difference $\Delta\overline{T}$ for all the local time and latitude intervals should include sufficient statistics to reveal possible temperature trends associated with increased levels of particle fluxes.

[14] During the 40 days in each data set, SABER does not sample the entire diurnal cycle. However, it provides fairly good coverage during the local nighttime for both seasons, which is favorable considering that we are interested in temperature measurement coinciding with significant particle fluxes as the particle precipitation in general is strongest on the nightside. This means that the $\Delta\overline{T}$ presented in this paper mainly represents the temperature difference found during early evening, nighttime, and early morning.

3.1. May/June 2003

[15] The period 22 May–30 June 2003 is characterized by both geomagnetic quiet and disturbed conditions as seen in the AE, Dst, and Kp index shown in Figure 1. The period also includes three solar proton events (SPEs). Figure 2 shows the average $\Delta\overline{T}$ profiles calculated for four different flux levels of particle precipitation. We do not find a statistically significant temperature increase at any altitude. However, above 100 km there seems to be a trend of elevated temperatures associated with strong fluxes of particle precipitation. Protons with energies in the range 30–80 keV deposit most of their energy between 110 and 140 km. The highest temperature increase associated with proton fluxes in this energy range is 15–20 K at 110 and 115 km.

[16] Protons with energies in the range 250–800 keV and electrons with energies >30 keV deposit most of their energies below 105 km. The two lower parts of Figure 2 focus on the altitude region 80–105 km. At and below 100 km, we do not find a consistent or statistically significant temperature response in either the temperatures associated with proton fluxes or the temperatures associated with electron fluxes.

3.2. October/November 2003

[17] The AE, Dst, and Kp indices for the period from 1 October–10 November are shown in Figure 3. From late October to early November, the period includes some extraordinary large geomagnetic storms, as well as three SPEs. Figure 4 shows the average $\Delta\overline{T}$ profiles calculated for four different levels of particle fluxes. We find a significant temperature increase at and above 110 km associated with strong fluxes of 30–80 keV and 80–250 keV protons. Additionally, there is a clear trend of increasing temperatures with increasing particle fluxes above 100 km. Focusing on the $\Delta\overline{T}$ profiles which coincide with large fluxes of 80–250 keV protons, we find a temperature increase of approximately 40 K at both 115 and 120 km in regions of high flux levels.

[18] The two lower parts of Figure 4 focus on the altitude region 80–105 km. We find a temperature increase at 100 km and 105 km associated with large proton and electron fluxes. However, at and below 95 km we do not find a consistent or statistically significant temperature response.

[19] In summary, the thermospheric temperature enhancements found in this study seem to be more pronounced in October/November compared to May/June. However,

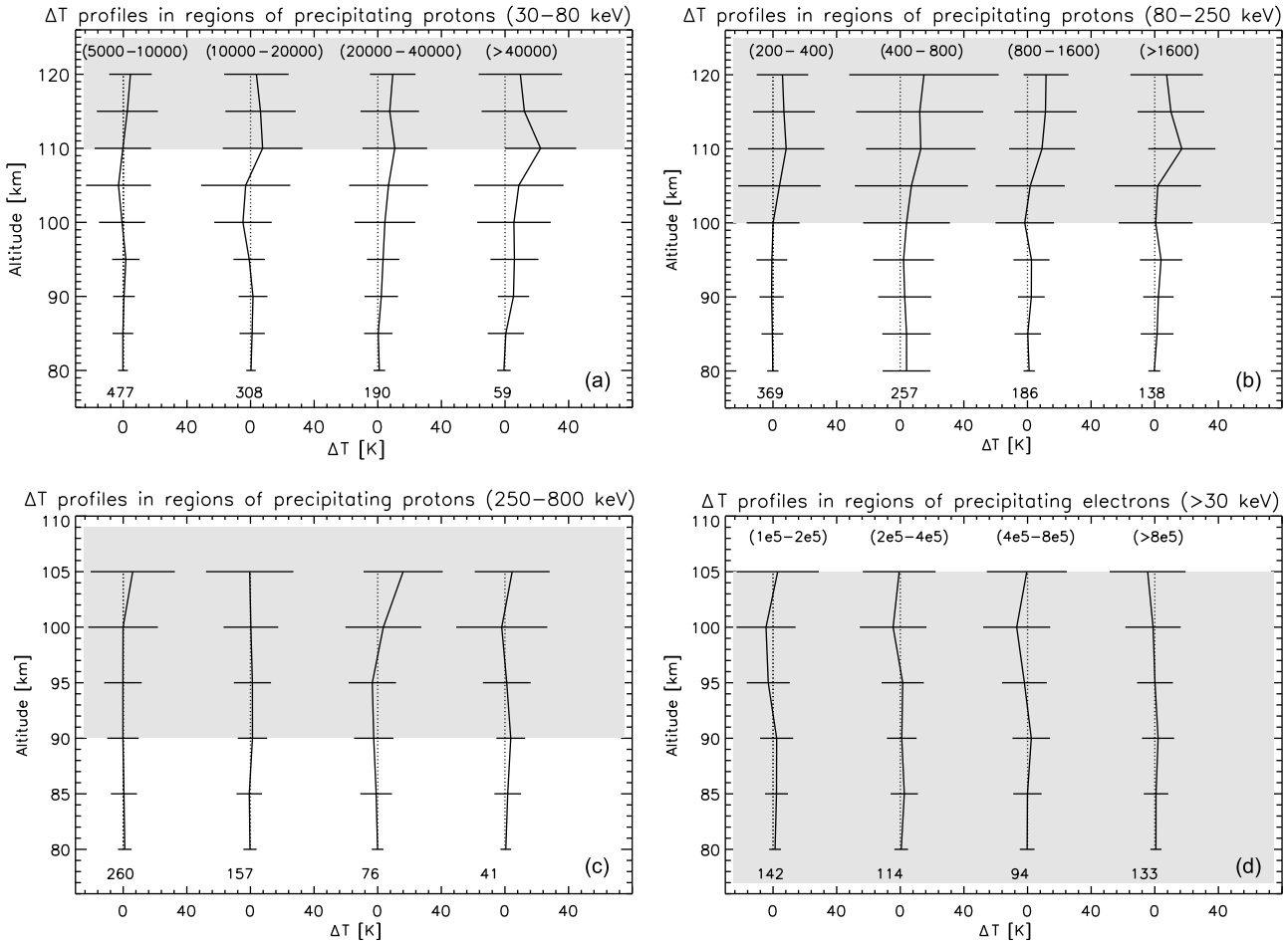

Figure 2. Average ΔT profiles ($\Delta\overline{T}$) for all local time hour intervals (1 hour) and geomagnetic latitude intervals (4°) in the period 22 May–30 June, 2003. The $\Delta\overline{T}$ profiles are given for four different intensity levels of protons 30–80 keV (a), 80–250 kev (b), 250–800 keV (c), electrons >30 keV (d). In each panel the flux level increases a factor of 2 from one ΔT profile to the next. The differential proton fluxes and integral electron fluxes have the units $(\text{cm}^2\ \text{s sr keV})^{-1}$ and $(\text{cm}^2\ \text{s sr})^{-1}$, respectively. The horizontal bars show the standard deviation of the ΔT profiles. The numbers written below the temperature profiles give the number of temperature measurements the average is based upon. The shaded regions mark the altitude interval where the particles deposit most of their energy.

neither time period reveals a consistent temperature trend below 100 km.

4. Discussion and Conclusion

[20] The main objective of this study is to investigate whether there are temperature effects in the upper mesosphere associated with energetic particle precipitation. The qualitative response of the lower thermosphere to geomagnetic disturbances is known to be heating [*Banks*, 1977; *Offermann*, 1985; *Lastovicka*, 1988]. Therefore, we may use the temperature response in the lower thermosphere to validate our method. The first part of this discussion is devoted to understanding the lower thermospheric temperature response to the particle precipitation. A more thorough evaluation of the lower thermospheric energy budget would require knowledge about the electrons and protons of energies less than 30 keV as well. In the second part of the discussion, we evaluate and compare our results in the upper mesosphere with previous studies.

4.1. The Lower Thermospheric Temperature Response

[21] During October/November, we found a temperature enhancement of ~40 K at 120 km associated with enhanced particle precipitation. Particle heating rates of more than 40 K/h are not unusual at 120 km [e.g., *Banks*, 1977]. It is also likely that Joule heating plays a significant role in the observed temperature increase, as the precipitating particles through ionization increase the Pedersen conductivity.

[22] Joule heating might also be one of the explanations for the different seasonal response observed in our statistical approach. The October/November data show a stronger and more consistent temperature response in the lower thermosphere compared to the May/June data. During May/June, Joule heating plays a more significant role during quiet conditions compared to October/November due to a larger Pedersen conductivity caused by solar irradiation [*Killeen et al.*, 1997]. The effect of the additional ionization caused by particle precipitation could therefore be relatively less during May/June compared to October/November, causing a

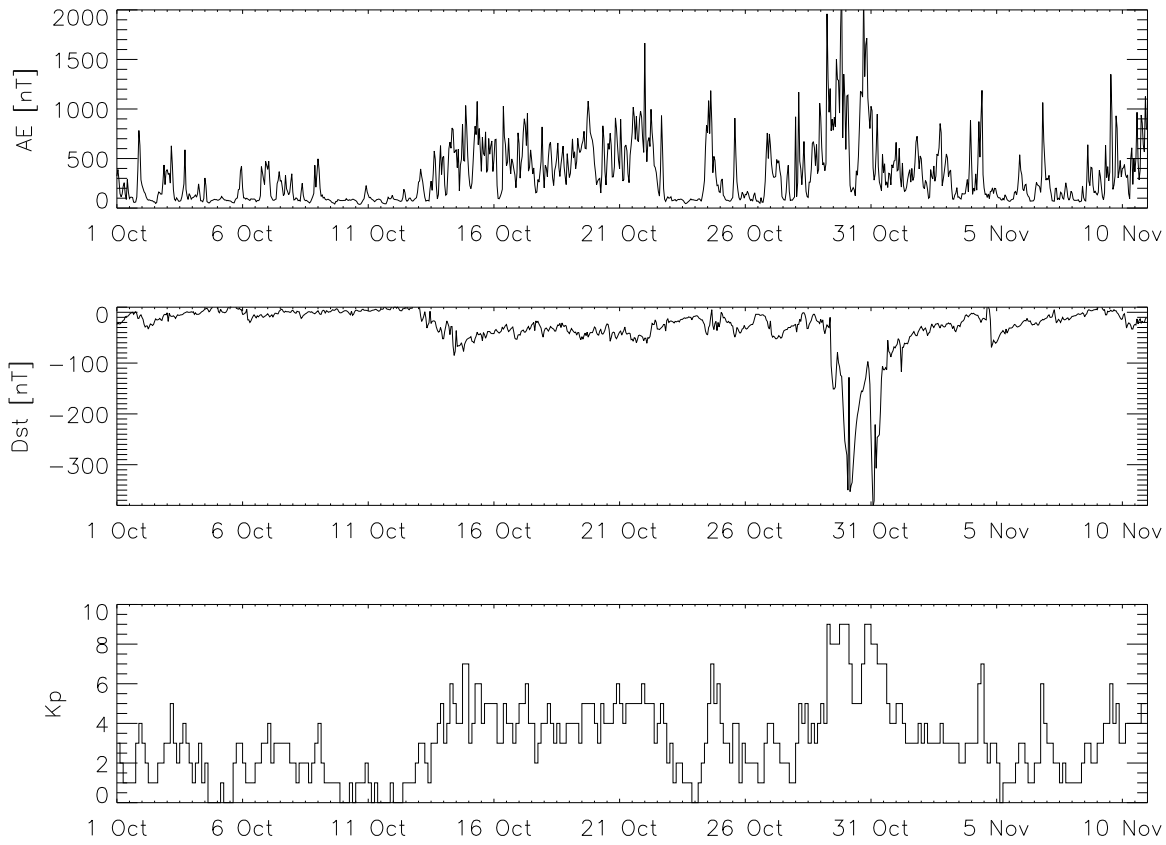

Figure 3. Hourly AE and Dst (upper and middle plot), and 3-hourly Kp (bottom plot) for the period 1 October–10 November 2003.

weaker correlation between particle precipitation and Joule heating.

[23] In general, we find that the temperature increase is more pronounced in regions of larger particle fluxes during both May/June and October/November as one should expect. However, the temperature response in the lower thermosphere does not increase linearly as a function of the particle flux. The temperature increase as a function of 80–250 keV proton fluxes for the October/November period is illustrated in Figure 5 for 110–120 km. We see that the temperature levels off as the flux increases. It seems almost as the temperature reaches a state of equilibrium where the atmosphere compensates for the additional heating by increasing the energy sinks. This is consistent with, e.g., a radiative cooling source such as infrared cooling by CO_2, which is proportional to the temperature gradient in the lower thermosphere [*Wintersteiner et al.*, 1992]. Joule and particle heating increases the temperature gradient and in this manner the CO_2 cooling rate.

[24] All in all, on the basis of the qualitative temperature response of the lower thermosphere, we believe that our method and data can be used to investigate whether there are significant temperature effects in the upper mesosphere associated with energetic particle precipitation.

4.2. The Upper Mesospheric Temperature Response

[25] *Pancheva et al.* [2007] found a temperature decrease of 25 K around 90 km in Northern Norway associated with the SPEs and geomagnetic storms in late October 2003. For the same event, model calculations by *Jackman et al.* [2007] showed a seasonal response where no significant temperature modification was found in the northern hemisphere, while a small heating effect of 2–3 K was found in the southern hemisphere. *von Savigny et al.* [2007] observed a temperature increase of a few K/d at about 86 km in the summer hemisphere coinciding with the January 2005 SPEs.

[26] In contrast to *von Savigny et al.* [2007], we did not find a consistent heating at and below 95 km coinciding with the energetic particle precipitation either during May/June or during October/November. Particle heating rates found by, e.g., *Banks* [1977] and *Offerman* [1985] during different geomagnetic disturbances were estimated to be just a few K/d around 90 km. Joule heating rates of a few K/d have also been found at these heights [*Banks*, 1979; *Roble et al.*, 1987]. The radiative relaxation times in the upper mesosphere are of the order of days [*Barabash et al.*, 2004], which suggest that a temperature modification can last for hours and days after an event. In other words, the temperature increase found by *von Savigny et al.* [2007] could be the accumulated heating caused by particle and Joule heating. Therefore, since we compare the temperature profiles only to the NOAA passes closest in time, we might not expect to see any temperature trends below 95 km. An accumulated heating effect or a possible cooling effect caused by, e.g., composition perturbations may require longer time scales to be observable. The temperature profiles in Figures 2 and 4 may be influenced by heating or cooling occurring hours prior to the SABER observations. Therefore, in Figure 6, we have

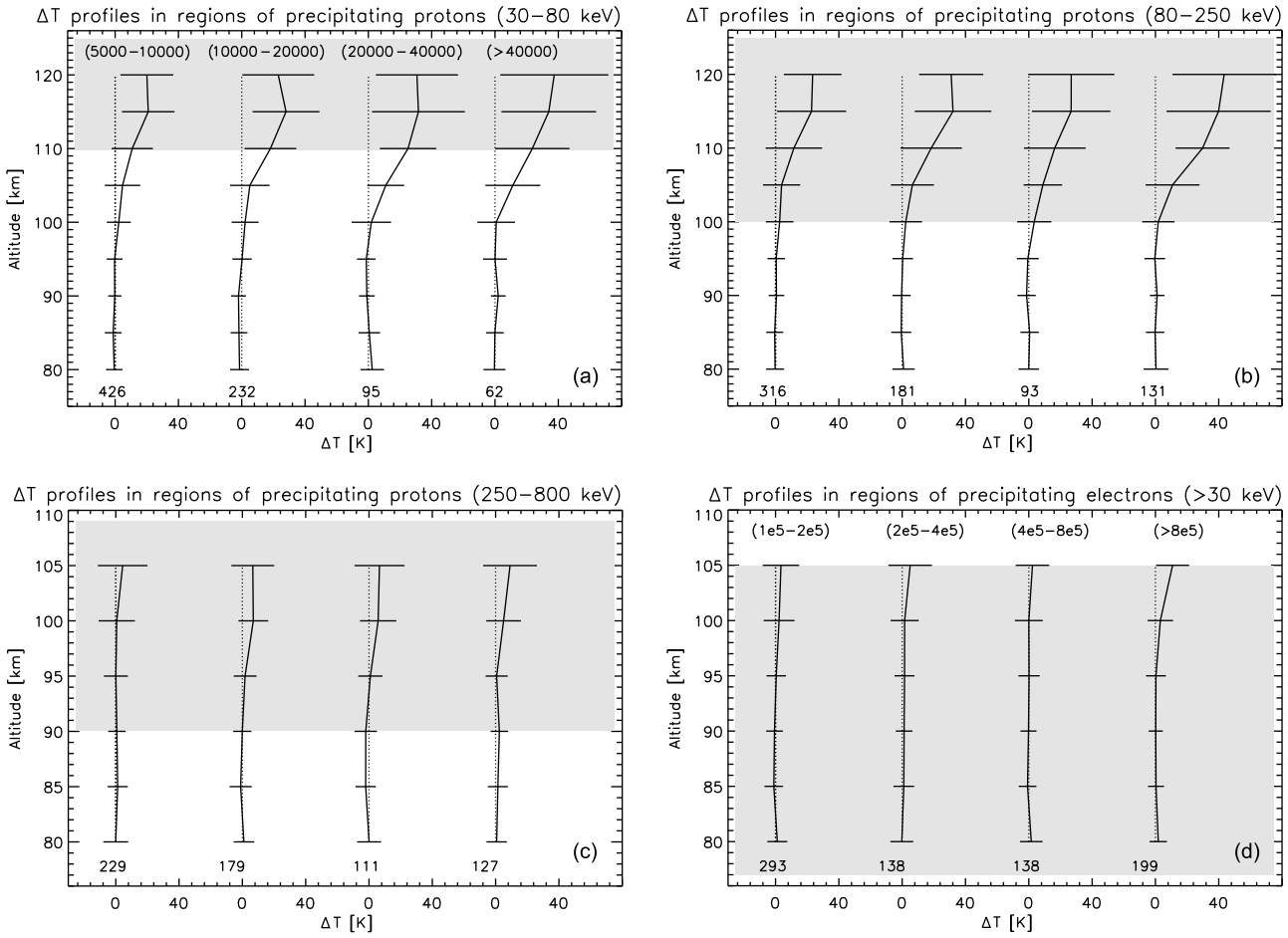

Figure 4. Same as Figure 2 for the period 1 October–10 November, 2003.

sorted the temperature profiles from the October/November period not only by the particle flux but also by the Kp indices measured during and prior to the observation. The dashed lines include all cases where the Kp index was less than or equal to 4 during the Kp interval of the temperature retrieval or in one of the preceding Kp intervals. The solid lines include all cases where the Kp index exceeded 4 during the Kp interval of the temperature retrieval and in both of the preceding Kp intervals. We see that there are some accumulated heating effects above 100 km. The temperatures retrieved in

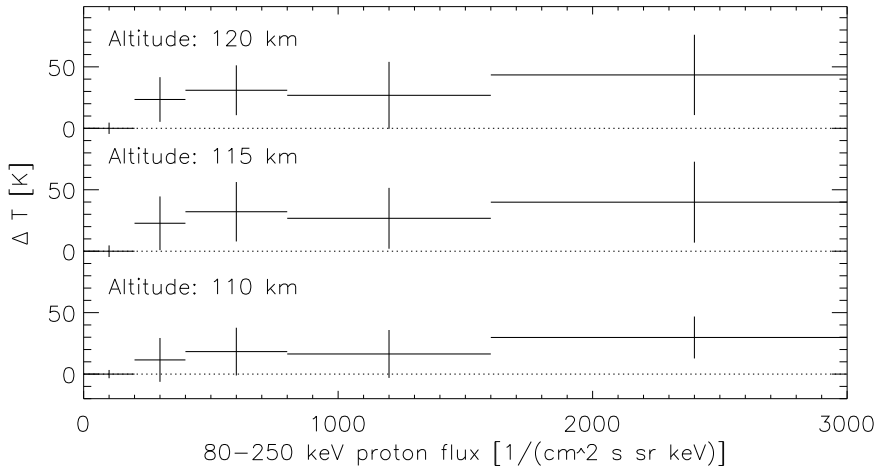

Figure 5. Average $\Delta\overline{T}$ associated with different fluxes of precipitating protons in the period 1 October–10 November 2003. The vertical bars show the standard deviation of the temperature profiles.

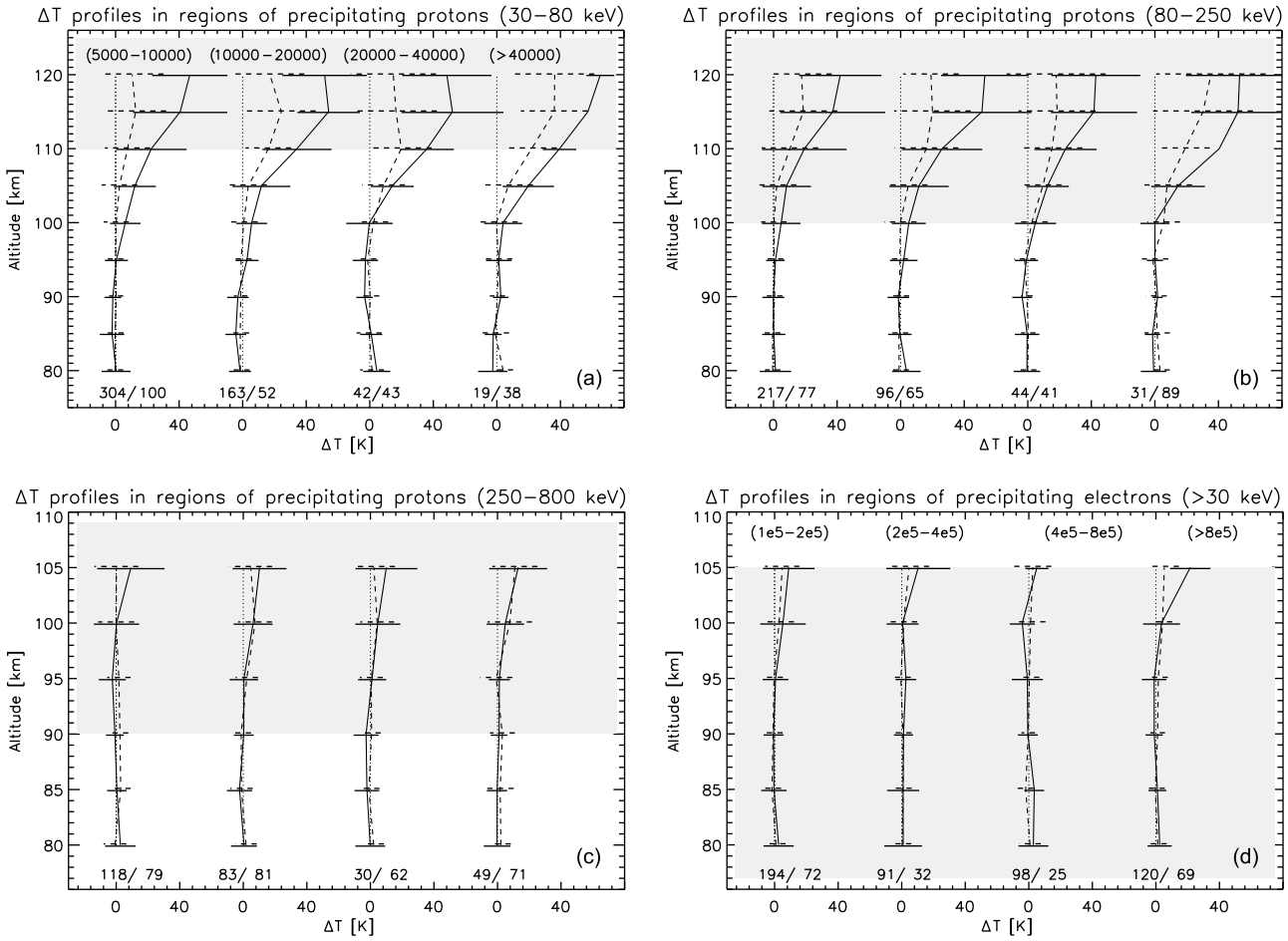

Figure 6. Same as Figure 4 with the ΔT profiles sorted according to the Kp values in addition to the particle fluxes. The dashed lines include all cases where the Kp index was less than or equal to 4 during or in one of the two Kp intervals prior to the temperature retrieval. The solid lines include all cases where the Kp index exceeded 4 during and in both of the two Kp intervals prior to the temperature retrieval. The numbers written below the temperature profiles give the number of temperature measurements the average is based upon. The first number is associated with the low Kp values, while the last number is associated with the high Kp values. The horizontal bars show the standard deviation of the temperature profiles.

periods of enhanced Kp values are in general larger than the temperatures retrieved in periods of low Kp values. In the upper mesosphere, the results are much more ambiguous as shown in the two lower plots in Figure 6. There is no apparent accumulated temperature trend below 100 km.

[27] In contrast to *Pancheva et al.* [2007], we did not find a consistent cooling trend below 100 km coinciding with regions of energetic particle precipitation. However, considering that the strong cooling observed by *Pancheva et al.* [2007] was based on ground-based observations associated with a specific region and local time, we should investigate whether there are any apparent local time or geomagnetic latitude dependencies in the temperature response. The color plot in Figure 7 shows the ΔT response at 85 km to proton fluxes in the energy range 250–800 keV at different geomagnetic latitudes and local times during October/November. As mentioned before, we do not have a complete local time coverage due to both the SABER sampling and that the particle precipitation in general is strongest on the nightside. Figure 7 shows regions and local times of both heating and cooling. From 16–19 LT we find a cooling trend at most geomagnetic latitudes. An apparent cooling trend is also found around local midnight at high latitudes and in the premidnight sector at lower latitudes. In fact, it turns out that most of the temperature profiles from these regions were measured in late October in the same period when *Pancheva et al.* [2007] observed the strong temperature decrease. Figure 8 shows the ΔT response at 85 km to proton fluxes in the energy range 250–800 keV at different local times in the period 27 October–6 November 2003. The general ΔT response is cooling. Figure 9 shows the average ΔT profiles retrieved in the period from 27 October–6 November 2003. The $\Delta\overline{T}$ values found in periods of low Kp values do not show a strong cooling or heating effect below 100 km. However, the $\Delta\overline{T}$ found in periods of high high Kp values appears to experience a cooling effect in the altitude interval 85 to 90 km with a maximum cooling of 3–4 K at 85 km. There is also a larger heating at and above 100 km.

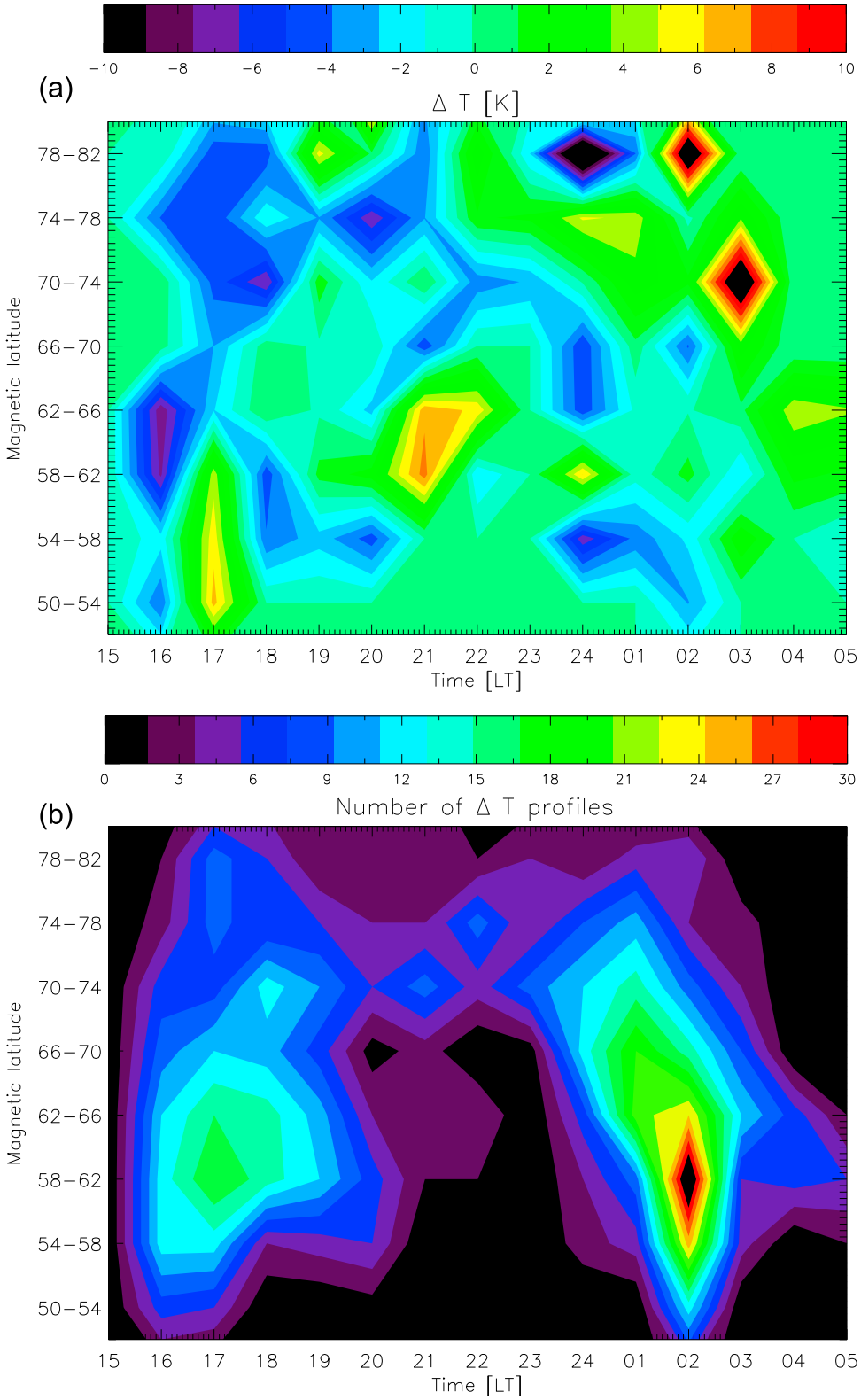

Figure 7. The upper plot is a contour plot of the ΔT response at 85 km to proton fluxes in the energy range 250–800 keV at different geomagnetic latitudes and local times during 1 October–10 November 2003. The ΔT is the difference between the average temperatures found in regions of fluxes larger and less than 5 $(cm^2\ s\ sr\ keV)^{-1}$. The lower plot shows the number of ΔT profiles the average are based upon.

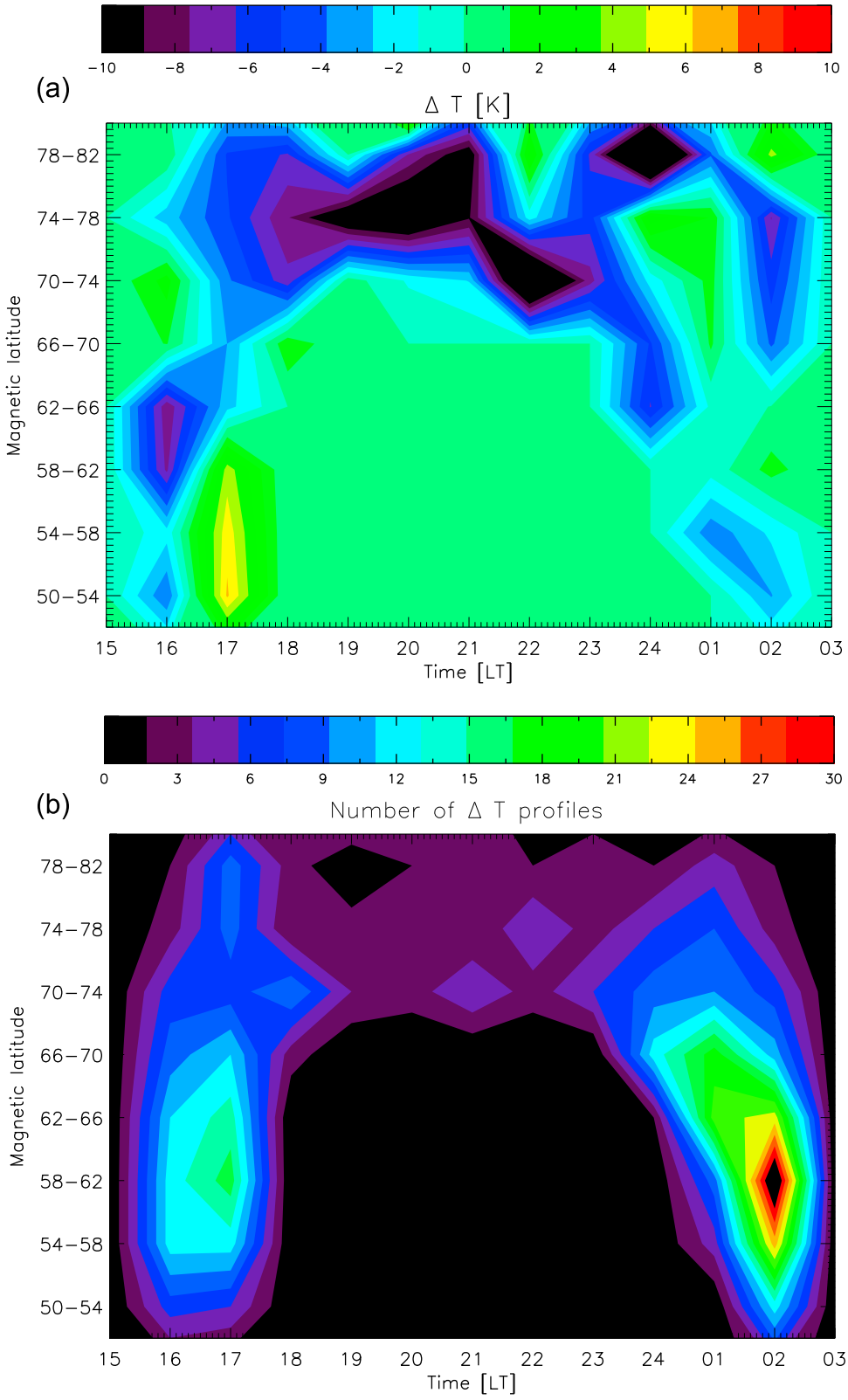

Figure 8. Same as Figure 7 for the period 27 October–6 November 2003.

[28] A possible temperature decrease around 90 km might give support to *Pancheva et al.* [2007]. A possible cooling effect could be initiated by the particle precipitation producing odd hydrogen species which could destroy ozone through catalytic processes [*Maeda and Aikin*, 1968; *Pesnell et al.*, 2000]. Ozone is important in absorption of solar ultraviolet radiation. Since we found our temperature drop mainly on the nightside, a possible reduction in the solar

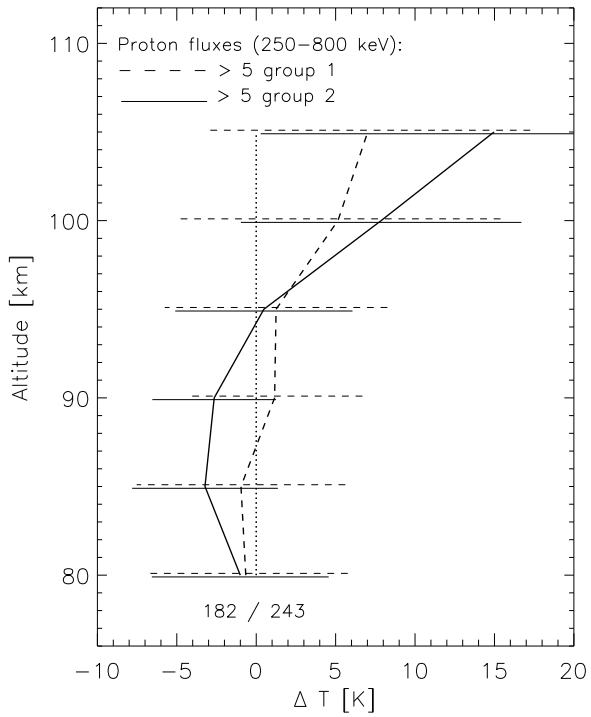

Figure 9. Average $\Delta\overline{T}$ based on SABER measurements in the period 27 October–6 November 2003. The dashed line includes all cases where the Kp index was less than or equal to 4 during or in one of the two Kp intervals prior to the temperature retrieval. The solid line includes all cases where the Kp index exceeded 4 during or in both of the two Kp intervals prior to the temperature retrieval. The numbers written below the ΔT profiles give the number of temperature measurements the average is based upon. The first number is associated with the low Kp values, while the last number is associated with high Kp values. The horizontal bars show the standard deviation of the ΔT profiles.

heating rates cannot be responsible for the observed temperature decrease. However, ozone also plays an important role in several exothermic reactions. In particular, the reaction with atomic hydrogen is important. Around midnight, a heating rate of 6 K/d can be provided by this reaction alone [*Mlynczak and Solomon*, 1991]. On the other hand, both hydrogen and ozone are affected by particle precipitation, and it is not evident how this affects the net heating rate. In addition to a possible reduction in the solar heating rates, *Pancheva et al.* [2007] suggested that the heating caused by precipitating protons below 90 km could cause upwelling of the air and consequently adiabatic cooling in the upper mesosphere. Usually, this dynamic response is located in the thermosphere, but *Pancheva et al.* [2007] suggested that the heating by the extraordinary solar proton fluxes in late October 2003 could cause a similar scenario in the mesosphere. The period studied is the fourth largest SPE in the past 40 years.

[29] In summary, on the basis of data from SABER on the TIMED satellite and MEPED detectors on NOAA, we have investigated the immediate temperature effects in the altitude range 80–120 km. During both May/June and October/November, we find trends of elevated temperatures above 100 km. Below 100 km, we do not find any consistent immediate temperature modification associated with the particle precipitation. Focusing on the extraordinary large geomagnetic storms and SPEs occurring in late October 2003, there might be a cooling effect in the altitude interval 80–90 km when considering temperatures retrieved during periods of enhanced Kp values.

[30] These first results encourage a future study where we could perform a more detailed study of the connection between the temperature and particle energy deposition at different height levels. We also want to integrate the particle energy deposition over successively longer time periods before the SABER temperature measurements to study possible accumulative effects on the temperature.

[31] **Acknowledgments.** This research was supported by the Research Council of Norway project 184701.

[32] Robert Lysak thanks the reviewers for their assistance in evaluating this paper.

References

Banks, P. M. (1977), Observation of Joule and particle heating in the auroral zone, *J. Atmos. Terr. Phys.*, *39*, 179–193.

Banks, P. M. (1979), Joule heating in the high-latitude mesosphere, *J. Geophys. Res.*, *84*, 6709–6712.

Barabash, V., S. Kirkwood, A. Feofilov, and A. Kutepov (2004), Polar mesosphere summer echoes during the July 2000 solar proton event, *Ann. Geophys.*, *22*, 759–771.

Evans, D. S., and M. S. Greer (2000), Polar Orbiting Environmental Satellite Space Environment Monitor 2: Instrument description and archive data documentation, *NOAA Tech. Memo., OAR SEC-93*, NOAA, Boulder, Colo.

Fang, X., M. W. Liemohn, J. U. Kozyra, D. S. Evans, A. D. Dejong, and B. A. Emery (2007), Global 30–240 keV proton precipitation in the 17–18 April 2002 geomagnetic storms: 1. Patterns, *J. Geophys. Res.*, *112*, A05301, doi:10.1029/2006JA011867.

Jackman, C. H., R. G. Roble, and E. L. Fleming (2007), Mesospheric dynamical changes induces by the solar proton events in October–November 2003, *Geophys. Res. Lett.*, *34*, L04812, doi:10.1029/2006GL028328.

Killeen, T. L., A. G. Burns, I. Azeem, S. Cochran, and R. Roble (1997), A theoretical analysis of the energy budget in the lower thermosphere, *J. Atmos. Terr. Phys.*, *59*, 675–689.

Lastovicka (1988), A review of solar wind and high energy particle influence on the middle atmosphere, *Ann. Geophys.*, *6*, 401–407.

Maeda, K., and A. C. Aikin (1968), Variations of polar mesospheric oxygen and ozone during auroral events, *Planet. Space Sci.*, *16*, 371–380, doi:10.1016/0032-0633(68)90153-0.

Mlynczak, M. G., and S. Solomon (1991), Middle atmospheric heating by exothermic chemical reactions involving odd-hydrogen species, *Geophys. Res. Lett.*, *18*, 37–40.

Nesse Tyssøy, H., D. Heinrich, J. Stadsnes, M. Sørbø, U.-P. Hoppe, D. S. Evans, B. P. Williams, and F. Honary (2008), Upper-mesospheric temperatures measured during intense substorms in the declining phase of the January 2005 solarproton events, *Ann. Geophys.*, *26*, 2515–2529.

Offermann, D. (1985), The energy budget campaign: introductory review, *J. Atmos. Terr. Phys.*, *47*, 1–26.

Pancheva, D., W. Singer, and P. Mukhatrov (2007), Regional response of the mesosphere-lower thermosphere dynamcis over Scandinavia to solar proton events and geomagnetic storms in late October 2003, *J. Atmos. Sol. Terr. Phys.*, *69*, 1075–1094.

Pesnell, W. D., R. A. Goldberg, C. H. Jackman, D. L. Chenette, and E. E. Gaines (2000), Variation of mesospheric ozone during the highly relativistic electron event in May 1992 as measured by the High Resolution Doppler Imager instrument on UARS, *J. Geophys. Res.105* 22,943–22,954, doi:10.1029/2000JA000091.

Rees, M. H., B. A. Emery, R. G. Roble, and K. Stamnes (1983), Neutral and ion gas heating by auroral precipitation, *J. Geophys Res.*, *88*, 6289–6299.

Roble, R. G., et al. (1987), Joule heating in the mesosphere and thermosphere during the July 13, 1982, solar proton event, *J. Geophys. Res.*, *92*, 6083–6090.

Roble, R. G. (1995), Energetics in the mesosphere and thermosphere, in *The Upper Mesosphere and Lower Thermosphere: A Review of Experiment and Theory*, *Geophys. Monogr. Ser.*, 87, 1–21.

von Savigny, S., M. Sinnhuber, H. Bovensmann, M.-B. Burrows, and M. Schwartz (2007), On the dissapearance of noctilucent clouds during the January 2005 Solar proton events, *Geophys. Res. Lett.*, *34*, L02805, doi:10.1029/2006GL028106.

Wintersteiner, P. P., R. H. Picard, R. D. Sharma, J. R. Winick, and R. A. Joseph (1992), Line-by-line radiative excitation model for the non-equilibrium atmosphere: Application to CO2 15-um emission, *J. Geophys. Res.*, *97*, 18,083–18,117.

Zadorozhny, A. M., V. N. Kikhtenko, G. A. Kokin, G. A. Tuchkov, A. A. Tyutin, A. F. Chizhov, and O. V. Shtirkov (1994), Middle atmosphere response to the solar proton events of October 1989 using the result of rocket measurements, *J. Geophys. Res.*, *99*, 21,059–21,069.

D. S. Evans, NOAA Space Environment Center, 325 Broadway, Boulder, CO 80305, USA.

C. J. Mertens, NASA Langley Research Center, Science Directorate, Chemistry and Dynamics Branch, 21 Langley Blvd., MS401B Hampton, VA 23681, USA.

J. Stadsnes and M. Sørbø, Department of Physics and Technology, University of Bergen, N-5007 Bergen, Norway.

H. Nesse Tyssøy, The Royal Norwegian Naval Academy, Pb 83 Haakonsvern N-5886 Bergen, Norway. (hilde.nesse@ift.uib.no)